ARTICLE

pubs.acs.org/Biomac

De Novo Designed Protein Transduction Domain Mimics from Simple Synthetic Polymers

A. Özgül Tezgel,[†] Janice C. Telfer,[‡] and Gregory N. Tew*[,†,‡]

[†]Department of Polymer Science and Engineering and [‡]Department of Veterinary and Animal Science, University of Massachusetts, Amherst, Massachusetts 01003, United States

Supporting Information

ABSTRACT: Protein transduction domains (PTDs) that readily transverse cellular membranes are of great interest and are attractive tools for the intracellular delivery of bioactive molecules. Learning to program synthetic polymers and oligomers with the appropriate chemical information to capture adequately the biological activity of proteins is critical to our improved understanding of how these natural molecules work. In addition, the versatility of these synthetic mimics provides the opportunity to discover analogs with superior properties compared with their native sequences. Here we report the first detailed structure−activity relationship of a new PTD family of polymers based on a completely abiotic backbone. The synthetic approach easily allows doubling the density of guanidine functional groups, which increases the transduction efficiency of the sequences. Cellular uptake studies on three different cell lines (HEK 293T, CHO, and Jurkat T cells) confirm that these synthetic analogs are highly efficient novel protein transduction domain mimics (PTDMs), which are more effective than TAT_{49-57} and nonaarginine (**R9**) and also highlight the usefulness of polymer chemistry at the chemistry−biology interface.

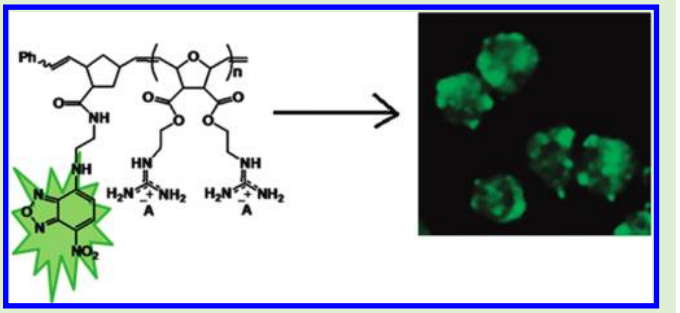

INTRODUCTION

Learning to design simple, synthetic structures that capture the biological activity of peptides, proteins, and oligonucleotides is an important challenge of modern macromolecular science. Building from our previous successes that focused on the design of synthetic antimicrobial peptide mimics,[1,2] we describe here the design, synthesis, and cellular internalization of an entirely new class of TAT-inspired protein transduction domain mimics (PTDMs). Although the interest in molecular transporters has remained high since the initial discovery of the HIV TAT protein more than 20 years ago, the ability to program chemically simple synthetic polymers with similar biological activity has only been recently reported.[3−6] Despite these initial reports, a detailed structure−activity relationship (SAR) correlating the chemical structures with transport activity has not been reported until now. The TAT-like PTDMs reported here are generated by the ring-opening metathesis polymerization (ROMP) of chemically functionalized strained bicyclic oxanorbornenes. (See Figure 1.) A fluorescence-activated cell sorter (FACS) was used as a tool to monitor the cellular internalization of dye-labeled molecules into HEK 293T, CHO, and Jurkat T cells, compared with the well-known standard nonaarginine, **R9**. The versatile synthetic platform also enabled an understanding of how polymer chain length and guanidine density impacted internalization efficiency.

In 1988, Frankel and Pabo[7] and Green and Lowenstein[8] independently reported that TAT protein from HIV is able to

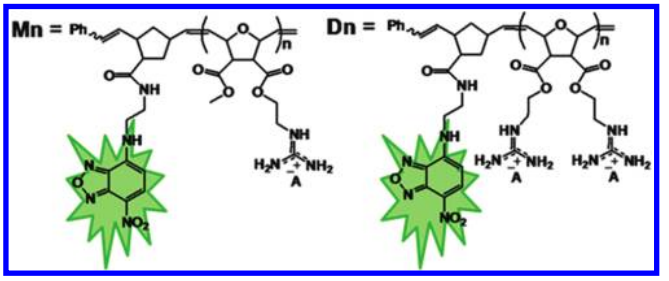

Figure 1. Structures of Methyl-(**Mn**) and Di-(**Dn**) guanidinium polymers.

cross cellular membranes and localize inside cells. Since then, the ability of these strongly cationic sequences to traverse the plasma membrane has been under intense study for two major reasons. First, it is well known that the plasma membrane limits the transport of highly charged molecules so the fact that these sequences, with multiple cationic centers, readily transverse the membrane is important for our fundamental understanding of membrane transport. This understanding has valuable implications in areas such as drug development. Second, the ability of these transporters or protein transduction domains (PTDs) to deliver cargo (proteins, antibodies, and nucleic acids) into

Received: May 23, 2011
Revised: May 27, 2011
Published: June 30, 2011

ACS Publications © 2011 American Chemical Society

mammalian cells offers possibilities for both new therapies and new tools to study cell biology.[9−11] PTDs primarily consist of cationic amino acid sequences like arginines, lysines, or both,[12−14] and early studies proved that the translocation abilities of PTDs were directly associated with the presence of arginine residues.[15−17] For example, in the case of TAT_{49-57} (RKKRRQRRR), replacement of the arginine amino acids with alanine or other cationic residues (lysine, histidine, and orthonine) led to reduced cellular uptake.[17] Substitution of all nonarginine residues with arginine (i.e., Arg-replacement) resulted in such enhanced internalization efficiency that **R9** was reported to be 20 times more efficient than TAT_{49-57}.[17] In addition to arginine content, the peptide length sets another parameter for cellular uptake; several groups showed that there is an optimum length for maximum activity.[15−18] In one instance, uptake efficiency increased as peptide length increased up to 15 amino acids, at which point longer peptides were less efficient.[15]

With this understanding of PTD activity as background, we designed, synthesized, and studied the cellular uptake properties of the guanidinium-rich structures shown in Figure 1. To track our polymers inside cells, they were labeled with a green fluorescent molecule, 7-chloro-4-nitrobenzo-2-oxa-1,3-diazole (NBD), by a postfunctionalization method.[19] Because most PTDs are relatively short sequences, the choice of dye molecule is important because it can significantly impact the overall molecular structure. Recently, the effect of fluorescein on cellular uptake and distribution of an octaarginine (R8) derivative was described. In the presence of the fluorescein tag, these R8 derivatives were observed in both the cytoplasm and nucleus; however, without fluorescein, only punctuate cytoplasmic staining was observed.[20] This is an illustrative example to show how the addition of a large dye molecule can easily alter the cellular uptake properties of a molecular transporter. NBD was chosen here because it is one of the smallest dyes available and therefore has a limited impact on the internalization activity of these polymers (Figure S28 of the Supporting Information).

In addition to evaluating the importance of chain length on internalization efficiency, this synthetic scaffold also allows us to study the effect of "guanidine density" on intracellular uptake in a way that previous structures could not. For example, Figure 1 shows two chemical structures, **Mn** and **Dn**, in which two sequences with the same chain length (n = degree of polymerization) were prepared, but those based on **Dn** have twice the density of guanidine groups as those based on **Mn**. Testing these newly designed PTDMs in three different cell lines, HEK293T, CHO, and Jurkat T cells, demonstrated that internalization was universal, whereas the best synthetic transporter showed a small dependence on cell type. Internalization assays at 4 °C highlighted the presence of energy- and temperature-independent pathways, implying that these PTDMs may be excellent delivery vectors because they avoid endosomal entrapment, which is known to decrease the efficiency and bioavailability of both the transporters and the cargo.[21,22] These results demonstrate that it is possible to introduce biological character into synthetic polymers so that they can act like PTDs and, in fact, are more efficient than one of the best peptides, **R9**.

EXPERIMENTAL SECTION

Synthesis of PTDMs. Monomers for PTDMs were prepared in three steps. The first step was the Diels−Alder reaction of maleic anhydride and furan. In the second step, the product from step 1 was reacted with the corresponding alcohol (methanol or 1,3-Di-Boc-2-(2-hydroxyethyl)guanidine), and the reaction was catalyzed by DMAP. Finally, 1,3-Di-Boc-2-(2-hydroxyethyl)guanidine was added to the monomer by EDC coupling. (See the Supporting Information for details.) Boc-protected guanidinine functionalized monomers were polymerized via Grubb's third-generation catalyst. (See the Supporting Information for details.)

Uptake of PTDMs. HEK293T and CHO cells were treated with 5 μM NBD-labeled PTDMs, and Jurkat T cells were treated with 2.5 μM NBD-labeled PTDMs for 30 min in complete growth medium supplemented with 10% fetal bovine serum. Then, the cellular uptake of the molecules was analyzed by fluorescence-activated cell sorter (FACS-BD-LSRII) or confocal microscopy (LSM510-Carl Zeiss, 40× oil immersion objective). (See the Supporting Information for details.)

RESULTS

Synthesis of NBD-Labeled Polymers. Di-Boc-protected guanidinium-functionalized monomers were synthesized in three steps[1] and resulted in ∼80% overall yield. (See the Supporting Information for details.) This synthetic monomer design allowed us to introduce one guanidinium group as a direct comparison to **R9** or two guanidinium groups, which doubled the functional group density. To visualize these PTDMs within cells, we end-labeled them by first ring-opening a succinimide-functionalized activated ester monomer,[19] then adding either the methyl or diguanidinium monomer units. Following polymerization, the succinimide ester was exchanged with an ethylenediamine-functionalized NBD dye, and the polymers were purified by both dialysis and column chromatography. The labeled polymers were characterized by NMR and UV-capable size exclusion chromatography. Analysis of the Boc-protected polymers yielded the expected molecular weights and narrow polydispersities (PDI ≈ 1.06 to 1.10), which are typical of ROMP because of its living nature.[26] In the last step, the Boc groups were removed using trifluoroacetic acid in dichloromethane. The final products were purified by dialysis and recovered by lyophilization. Although ester groups present in the polymers could undergo hydrolysis, it was not expected to impact the experimental results because the time scale of these in vitro experiments is short (∼30 min) compared with the room-temperature stability in buffer (PBS, pH 7.2) (>2 weeks); hydrolysis in the presence of cells has therefore not been investigated to date.

Cellular Uptake Assays. To avoid artifacts from the cellular uptake experiments, several precautions were taken. Previous studies on PTDs documented artifacts that result from cells being fixed prior to quantification.[24,27] Therefore, cell fixation, which is unnecessary, was not used. Furthermore, to measure only the fluorescence from internalized molecules, we employed the NBD-dithionite assay to quench any cell-surface-bound fraction remaining after the last washing step.[23] After quenching the cell-surface-bound molecules, NBD-labeled molecules were detected in >80% of the cells at 5 μM, as shown in Figure 2a by a representative FACS histogram. The relative internalization efficiency of NBD-labeled molecules was demonstrated using both the mean fluorescence per cell and percent cellular uptake. Figure 2b shows the impact of **Dn** polymer length comparing the mean fluorescence between cell-associated (prior to dithionite treatment, open bars) and internalized molecules (following surface bound NBD quenching, closed bars).

As the PTDM length increased, the number of both internalized and cell-surface-bound molecules increased. For

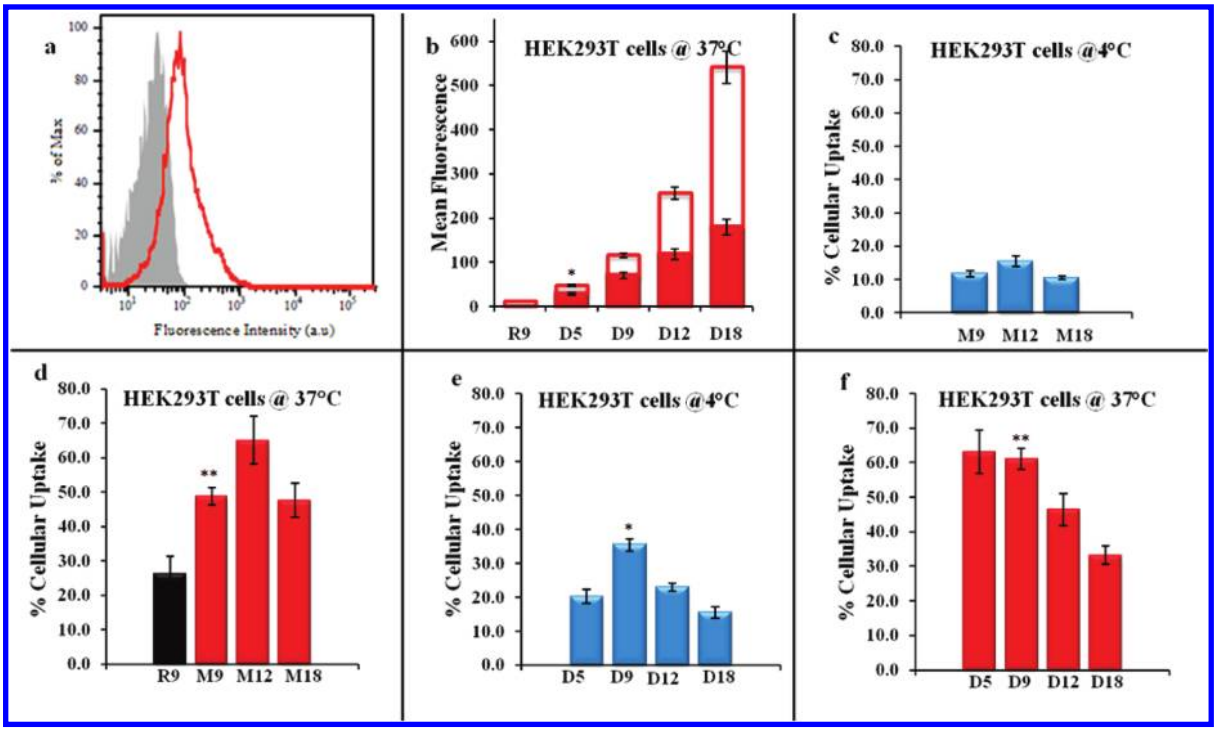

Figure 2. Internalization of molecules in HEK293T cells. (a) Representative FACS histogram showing the cellular uptake of 5 μM NBD-labeled **D9** molecule at 37 °C after treatment with the NBD/dithionite assay. The solid gray curve is untreated HEK293T cells; the red line represents cells treated with **D9**. (b) HEK293T cells were treated with diguanidinium polymers (**D5**, **D9**, **D12**, **D18**) at 37 °C. The amount of surface-bound and internalized molecules was determined by the NBD/dithionite assay. The amount of molecules bound to the surface (open bars) was obtained by subtracting the amount of internalized PTDMs (closed bars) from the total mean fluorescence intensity. The mean fluorescence of internalized polymers (after quenching the cell surface bound fraction of polymers by dithionite) was divided by the total mean fluorescence (before dithionite quenching) and multiplied by 100 to obtain the percent cellular uptake.*($P < 0.05$) of **D5** versus **R9** mean fluorescence at 37 °C. Translocation of polymers was represented as the percentage of internalization in HEK293T cells treated with 5 μM NBD-labeled nonaarginine (**R9**) control and methyl-guanidinium polymers (**Mn**) (c) at 4 °C and (d) at 37 °C. **($P < 0.01$) of **M9** versus **R9** percent cellular uptake. (e) Percent cellular uptake in HEK293T cells treated with 5 μM NBD-labeled diguanidinium polymers (**Dn**) at 4 °C, *($P < 0.05$) of **D9** versus **D18** percent cellular uptake and (f) at 37 °C, and **($P < 0.01$) of **D9** versus **D18** percent cellular uptake. Each point is the mean ± SD of three separate determinations.

example, **D18** is twice as long as **D9**, and **D18** is two times more efficient than **D9** in terms of the internalized fluorescence intensity. However, there is a ten-fold increase in the cell-surface-bound fraction, indicating that **D18** interacts with the cell surface much more strongly than **D9**, but it is not internalized as efficiently. The mean fluorescence intensity of internalized molecules provides information regarding the uptake of molecules; however, more information is needed to develop a detailed SAR for PTDMs that efficiently cross the plasma membrane.

In the simplest form of this process (ignoring biological processes like endocytosis), there are at least two important, yet different, equilibrium constants that need to be considered: ratio of PTDM in solution to cell-surface-bound PTDM and ratio of cell-surface-bound PTDM to internalized PTDM. Because of our interest in the second process, the data have been normalized as the percent cellular uptake, which is the percent ratio of internalized molecules (following dithionite treatment) to total cell associated molecules (before dithionite treatment). (See the Supporting Information for details.) This ratio is conceptually demonstrated in Figure 2b by the solid and open red bars for each PTDM. This normalized then allows direct comparisons to be made among all PTDMs and across all cell types. This method was chosen to present the data because the ratio is a more accurate way to understand the internalization efficiency of each PTDM and because it separates internalization from cell-surface-binding affinity. This would be unnecessary if every molecule had the same affinity for the cell surface, but as shown by the mean fluorescence data, this is not true. As a result, despite the identical concentrations in solution, the concentration at the cell surface varies with molecular structure and cell type. Therefore, the Figures after Figure 2b report the percent cellular uptake, focusing on the PTDMs that are the most efficient at crossing the membrane.

Initially, the PTDMs **Mn** and **Dn**, with various molecular weights, were evaluated for uptake in HEK293T cells (Figure 2) along with the control **R9**. These data clearly demonstrate that the methyl and diguanidinium polymers were able to function as PTDMs and, in fact, showed greater internalization efficiency than the thoroughly studied control **R9**.[15−17] Within the **Mn** series, the maximum efficiency was observed with 12 repeat units (**M12**) when compared with 9 (**M9**) and 18 (**M18**) (Figure 2d). In the **Dn** series, which has double the number of guanidinium groups compared with the **Mn** series, the most efficient PTDMs have lengths of 5 and 9 repeat units (**D5** and **D9**, respectively) (Figure 2f). The fact that **D5**, **D9**, and **M12** show similar internalization efficiencies suggests that the number of guanidinium groups is not the only factor affecting cellular uptake and that the density of guanidinium groups also plays an important role. Experiments were also conducted at 4 °C (Figure 2c,e) to

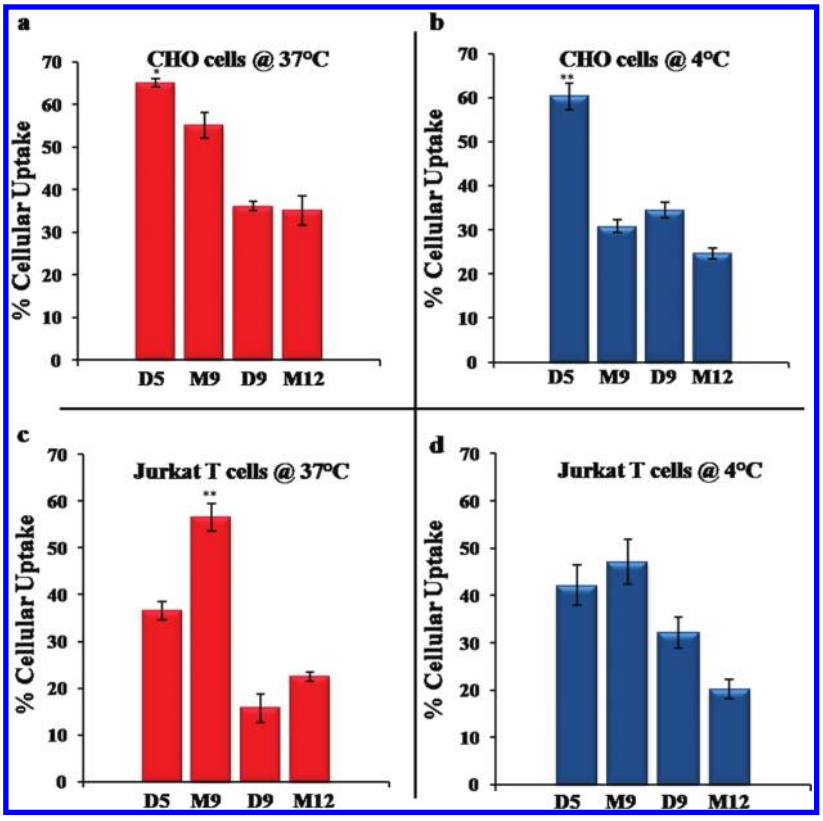

Figure 3. Percent cellular uptake of NBD-labeled polymers in (a,b) CHO and (c,d) Jurkat T cells at 37 and 4 °C. CHO cells were incubated with 5 μM NBD-labeled polymers (a) at 37 °C, *($P < 0.05$) of **D5** versus **M9** percent cellular uptake, and (b) at 4 °C, **($P < 0.01$) of **D5** versus **M9** percent cellular uptake. Jurkat T cells were treated with 2.5 μM NBD-labeled polymers (c) at 37 °C, **($P < 0.01$) of **M9** versus **D5** percent cellular uptake, and (d) at 4 °C. For the calculation of % internalization, experiments were done with dithionite-quenched and without dithionite-treated cells, and the percent ratio of internalization represents the transduction efficiency of the molecules. Each point is the mean ± SD of three separate determinations.

inhibit energy-dependent pathways. Experiments at 37 °C showed that the guanidinium density affects the internalization, and the experiments at 4 °C demonstrated this even more clearly. As shown in Figure 2c,e, at lower temperature, **Dn** molecules are even more efficient than their **Mn** analogues. For example, **D9** showed 35% cellular uptake compared with 10% for **M18**, although the total number of guanidinium groups is the same. Among all PTDMs, **D9** showed superior uptake at 4 °C, making it the most favorable molecule for internalization by nonendocytotic pathways (Figure 2e).

In addition to cellular uptake experiments at 37 and 4 °C, cytotoxicity testing was performed using 7-amino-actinomycin D (7-AAD) viability dye to determine lethal concentrations (LC_{50}). To build an SAR, plots were made of percent cellular uptake versus LC_{50}, and the graph was divided into four quadrants (Figure S25 of the Supporting Information). Optimal PTDMs would be those structures with high internalization efficacy and high LC_{50} values or low toxicity (quadrant II). All of the molecules in quadrants I and II in Figures S25a and S25b of the Supporting Information were considered to be promising PTDMs for further study because they showed both low toxicity and good cellular uptake. In addition, all of the PTDMs reported here showed no toxicity in the working concentration range.

To expand the cell types examined, we evaluated the PTDMs specified as most effective in HEK293T cells for internalization in both CHO and Jurkat T cells. Figure 3a shows that in CHO cells the shorter PTDMs, **D5** and **M9**, were more efficient than their longer analogs, **D9** and **M12**. **D9** and **M12** were found to adsorb more strongly on the cell membrane, but their ability to enter the cells was limited with internalization efficiencies near 35% compared with **M9** and **D5**, which had efficiencies of 55 and 65%, respectively. PDTM **D5** demonstrated remarkable uptake in this cell type at both temperatures, in contrast with its lower uptake in HEK293T cells at 4 °C. The addition of eight more guanidinium groups (in the case of **D9**) did not increase the uptake in CHO cells at 37 or 4 °C but, in fact, reduced the percent of internalized molecules while enhancing the cell surface binding compared with **D5**. Furthermore, **M9** and **D5** have essentially the same number of guanidinium groups and exhibited similar uptake characteristics at 37 °C (Figure 3a). Nevertheless, **D5** remained the best in class with a slightly higher internalization percentage at 37 °C and a significantly higher internalization percentage at 4 °C (60 vs 30%). Similar to the observations with the HEK293T cells, the **Dn**-series PTDMs entered CHO cells more efficiently at 4 °C than the **Mn**-series.

Jurkat T cells were found to be more sensitive to changes in the density of guanidinium group and the chain length. For example, **D9** and **M12** demonstrated considerable toxicity, even at low concentrations like 5 μM. As a result, and in contrast with the other cell studies, all of the uptake studies with these suspension cells were performed at a lower concentration of 2.5 μM. The shorter sequences, **D5** and **M9**, remained more efficient, showing better uptake profiles at both high and low temperatures (Figures 3c,d), whereas **D9** and **M12** showed a high affinity for

the cell surface. (See Figures S21 and S22 of the Supporting Information.). In this T cell line, **M9** exhibited outstanding uptake at 37 °C (60%), which was slightly diminished at 4 °C (50%), yet still comparable to **D5**. The importance of increased guanidinium density (**Dn** vs **Mn**) is emphasized at 4 °C as the percent cellular uptake of **D5** remained 40% at both 37 and 4 °C, whereas the uptake of **M9** decreased from 60 to 50% upon reducing the temperature. **D9** was more efficient at 4 °C than at 37 °C (32 vs 16%), showing the importance of guanidinium density on the energy-independent internalization pathway.

Although the detailed mechanism of cellular internalization is beyond the scope of this Article, some insight into the cellular location of these PTDMs is warranted. The internalization efficiency at 37 °C compared with 4 °C implies that energy-independent mechanisms are operative with these novel, synthetic PTDMs. To further explore their internalization, we visualized the presence of **D9** in CHO cells using confocal microscopy. As shown in Figure 4a, all of the cells within the field contain significant green fluorescence from the NBD-labeled PTDM. Simultaneously, LysoTracker Red DND-99 was employed to stain endosomic vesicles present in these CHO cells, as shown in Figure 4b, and the overlaid image (Figure 4c) shows yellow areas where **D9** and LysoTracker Red DND-99 are colocalized in the endosomes/lysosomes. Figure 4c also shows uniform diffuse green cytoplasmic staining within the cell, indicating the presence of **D9** outside of endosomic vesicles.

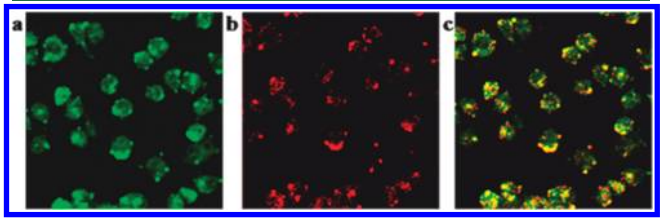

Figure 4. Localization of D9 polymers in CHO cells. CHO cells were incubated with 5 μM NBD-labeled **D9** polymer for 60 min at 37 °C after the last washing step cells were subsequently incubated with Lysotracker red-99 for 4 min, washed, and placed in ice-cold HBSS buffer. (a) Localization of **D9** molecules (green channel), (b) localization of Lysotracker red-99 (red channel), and (c) colocalization of **D9** molecules and lysotracker (overlay). Note that all cells have a uniform green background, demonstrating that **D9** is present outside of lysosome/endosomes.

DISCUSSION

Arginine-rich structures are known to translocate across the plasma membrane.[8−13] The aim of this work was to demonstrate that it is possible to program synthetic polymers to behave like natural PTDs. Using ROMP, novel sequences were designed to study the SAR between guanidinium functionalized polymers and cellular internalization in three different cell types. ROMP was chosen because it is well known to be functional-group-tolerant, and it is a living polymerization method that allows the number-average degree of polymerization to be narrowly defined and easily controlled. Here we introduced two novel structural classes of new PTDMs, **Mn** and **Dn**. These two structural classes allow us to distinguish total charge density or the total number of guanidinium functions from molecular length. For example, within the group **M9**, **D5**, and **D9**, one can compare the number of guanidines (**M9** vs **D5**) or the total length (**M9** vs **D9**). (See Figure 5.) Specifically, the ability to prepare peptides with the same overall length but twice the functional group density is nontrivial. Whereas cationic sequences can be cytotoxic, 7-AAD assays determined that all internalization studies were conducted below any concentrations that influenced cell viability.

To better analyze the internalization efficiencies of these PTDMs and their affinities for the cell membrane, the fluorescence from cell-surface-bound molecules was quenched using the established NBD-dithionite assay and data collected for both treated and untreated cells. We report percent cellular uptake, the ratio of mean fluorescence intensity per cell from cell populations treated with dithionite (only internalization fluorescence) to cells not treated with dithionite (both internal and surface-bound fluorescence). This highlights the important parameters related to the transport ability of these PTDMs. By examining this percent cellular uptake rather than simply mean fluorescence per cell for each molecule, a more direct measure of internalization efficiency is obtained because the raw data clearly show that some structures bind to the cellular surface more strongly, and, as a result, the concentration of PTDMs at the surface are proportionally higher.

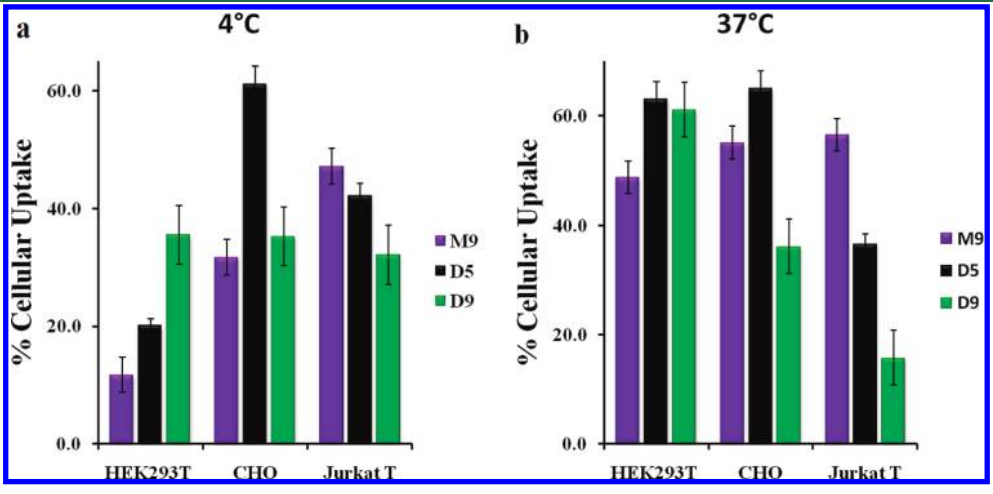

Figure 5. Comparison of the percent cellular uptake of NBD-labeled **M9**, **D5**, and **D9**, in HEK293T, CHO, and Jurkat T cells at (a) 4 and (b) 37 °C. HEK293T and CHO cells were incubated with 5 μM NBD-labeled polymers, and Jurkat T cells were incubated with 2.5 μM NBD-labeled polymers. For the calculation of % internalization, experiments were done with dithionite-quenched and without dithionite-treated cells, and the percent ratio of internalization represents the transduction efficiency of the molecules. Each point is the mean ± SD of three separate determinations.

In addition, the internalization mechanism of arginine-rich PTDs has been reported as mainly endocytosis in which the encapsulation in endocytotic vesicles is a major restriction to the use of these peptides in cytosolic-, nuclear-, and organelle-specific delivery.[21,22] In the case of endocytotic pathways, transporter molecules are trapped inside endosomes/lysosomes in an environment with an acidic pH and digestive enzymes that inhibit the capability of transporter molecules to deliver their cargo. To explore the internalization of these novel PTDMs, we examined uptake at 37 and 4 °C as well as by microscopy and colocalization with lysotracker red-99. Internalization was generally higher at 37 than 4 °C, which is consistent with the literature and a reasonable observation because endocytotic pathways would be operative. This is confirmed by the microscopy studies shown in Figure 4. However, and importantly, significant internalization is observed at 4 °C, demonstrating that these novel PTDMs also exploit energy-independent pathways. In the **Dn** series, percent cellular uptake for CHO and Jurkat T-cells is generally similar at 37 and 4 °C, indicating that these PTDMs efficiently access energy- and temperature-independent pathways. (See Figure 3.) It should be noted that in Jurkat T-cells **D9** is twice as efficient at 4 °C compared with 37 °C; this highlights the role of polymer chemistry and demonstrates the importance of establishing a SAR. In agreement with this observation is the fact that the overlaid image in Figure 4c shows distinct regions of only green emission associated with the presence of PTDMs outside of endosomes. This improved uptake of the **Dn** PTDMs, especially at 4 °C, implies that not only the presence but also the density of guanidine units influences uptake pathways and that a greater density of guanidine units can optimize internalization via energy- and temperature-independent pathways. The fact that the best-in-class PTDM varies among cell lines is to be expected[25]and further demonstrates the value of this versatile synthetic platform. For example, examining percent cellular uptake at 37 °C shows that **D5** and **D9** are better than **M9** in HEK293T cells, whereas **D5** is better than **M9** and **D9** in CHO cells but **M9** is superior in Jurkat T cells (Figure 5).

In conclusion, we have shown that synthetic polymers can be easily modified to mimic natural PTDs by introducing the appropriate functionality. Also, these synthetic structures demonstrated superior uptake efficiencies compared with a well-known peptide analogue and allowed us to determine the critical parameters for cellular internalization, especially for energy-independent internalization. Taken together, these synthetic analogs are highly efficient novel transporter molecules and promising tools for the delivery of bioactive macromolecules, highlighting the usefulness of polymer chemistry at the chemistry—biology interface.

■ ASSOCIATED CONTENT

Ⓢ Supporting Information. Experimental details (monomer and polymer synthesis as well as cellular uptake studies). This material is available free of charge via the Internet at http://pubs.acs.org.

■ AUTHOR INFORMATION

Corresponding Author
*E-mail: tew@mail.pse.umass.edu.

■ ACKNOWLEDGMENT

This work was supported by a grant from the National Science Foundation (CHE-0910963).

■ REFERENCES

(1) Lienkamp, K.; Madkour, A. E.; Musante, A.; Nelson, C. F.; Nusslein, K.; Tew, G. N. *J. Am. Chem. Soc.* **2008**, *130*, 9836–9843.
(2) Gabriel, G. J.; Madkour, A. E.; Dabkowski, J. M.; Nelson, C. F.; Nüsslein, K.; Tew, G. N. *Biomacromolecules* **2008**, *9*, 2980–2983.
(3) Hennig, A; Gabriel, G. J.; Tew, G. N.; Matile, S. *J. Am. Chem. Soc.* **2008**, *130*, 10338–10344.
(4) Kolonko, E. M.; Kiessling, L. L. *J. Am. Chem. Soc.* **2008**, *130*, 5626–5627.
(5) Kolonko, E,M.; Pontrello, J. K.; Mangold, S. L.; Kiessling, L. L. *J. Am. Chem. Soc.* **2009**, *131*, 7327–7333.
(6) Cooley, C. B.; Trantow, B. M.; Nederberg, F.; Kiesewetter, M. K.; Hedrick, J. L.; Waymouth, R. M.; Wender, P. A. *J. Am. Chem. Soc.* **2009**, *131*, 16401–16403.
(7) Frankel, A. O.; Pabo, C. O. *Cell* **1988**, *55*, 1189–1193.
(8) Green, M.; Lowenstein, P. M. *Cell* **1988**, *55*, 1179–1188.
(9) Fonseca, S. B.; Pereira, M. P.; Kelley, S. O. *Adv. Drug Delivery Rev.* **2009**, *61*, 953–964.
(10) Gump, J. M.; Dowdy, S. F. *Trends Mol. Med.* **2007**, *13*, 443–448.
(11) Sebbage, V. *Biosci. Horiz.* **2009**, *2*, 64–72.
(12) Schwarze, P. M.; Dowdy, S. F. *Trends Pharmacol. Sci.* **2000**, *21*, 45–48.
(13) Futaki, S.; Goto, S.; Sugiura, Y. *J. Mol. Recognit.* **2003**, *16*, 260–264.
(14) Fischer, P. M.; Zhelev, N. Z.; Wang, S.; Melville, J. E.; Fåhraeus, R.; Lane, D. P. *J. Peptide Res.* **2000**, *55*, 163–172.
(15) Mitchell, D. J.; Kim, D. T.; Steinman, L; Fathman, C. G.; Rothbard, J. B. *J. Peptide Res.* **2000**, *56*, 318–325.
(16) Futaki, S.; Suzuki, T.; Ohashi, W.; Yagami, T.; Tanaka, S.; Ueda, K.; Sugiura, Y. *J. Biol. Chem.* **2001**, *276*, 5836–5840.
(17) Wender, P. A.; Mitchell, D. J.; Pattabiraman, K.; Pelkey, E. T.; Steinman, L.; Rothbard, J. B. *Proc. Natl. Acad. Sci. U.S.A.* **2000**, *97*, 13003–13008.
(18) Rothbard, J. B.; Kreider, E.; VanDeusen, C. L.; Wright, L.; Wylie, B. L.; Wender, P. A. *J. Med. Chem.* **2002**, *45*, 3612–3618.
(19) Roberts, S. K.; Sampson, N. *Org. Lett.* **2004**, *63*, 253–3255.
(20) Puckett, C. A.; Barton, J. K. *J. Am. Chem. Soc.* **2009**, *131*, 8738–8739.
(21) Cheung, J. C.; Chiaw, P. K.; Deber, C. M.; Bear, C. E. *J. Controlled Release* **2009**, *137*, 2–7.
(22) Abes, S.; Williams, D.; Prevot, P.; Thierry, A.; Gait, M. J.; Lebleu, B. *J. Controlled Release* **2006**, *110*, 595–604.
(23) Drin, G.; Cottin, S.; Blanc, E.; Rees, A. R.; Temsamani, J. *J. Biol. Chem.* **2003**, *278*, 31192–31201.
(24) Jones, S. W.; Christison, R.; Bundell, K.; Voyce, C. J.; Brockbank, S. M. V.; Newham, P.; Lindsay, M. A. *Br. J. Pharmacol.* **2005**, *145*, 1093–1102 .
(25) Mueller, J.; Kretzschmar, I.; Volkmer, R.; Boisguerin, P. *Bioconjugate Chem.* **2008**, *19*, 2363–2374.
(26) Choi, T. L.; Grubbs, R. H. *Angew. Chem., Int. Ed.* **2003**, *42*, 1743–1746.
(27) Thorén, P. E.; Persson, D.; Isakson, P.; Goksör, M.; Onfelt, A.; Nordén, B. *Biochem. Biophys. Res. Commun.* **2003**, *307*, 100–107.